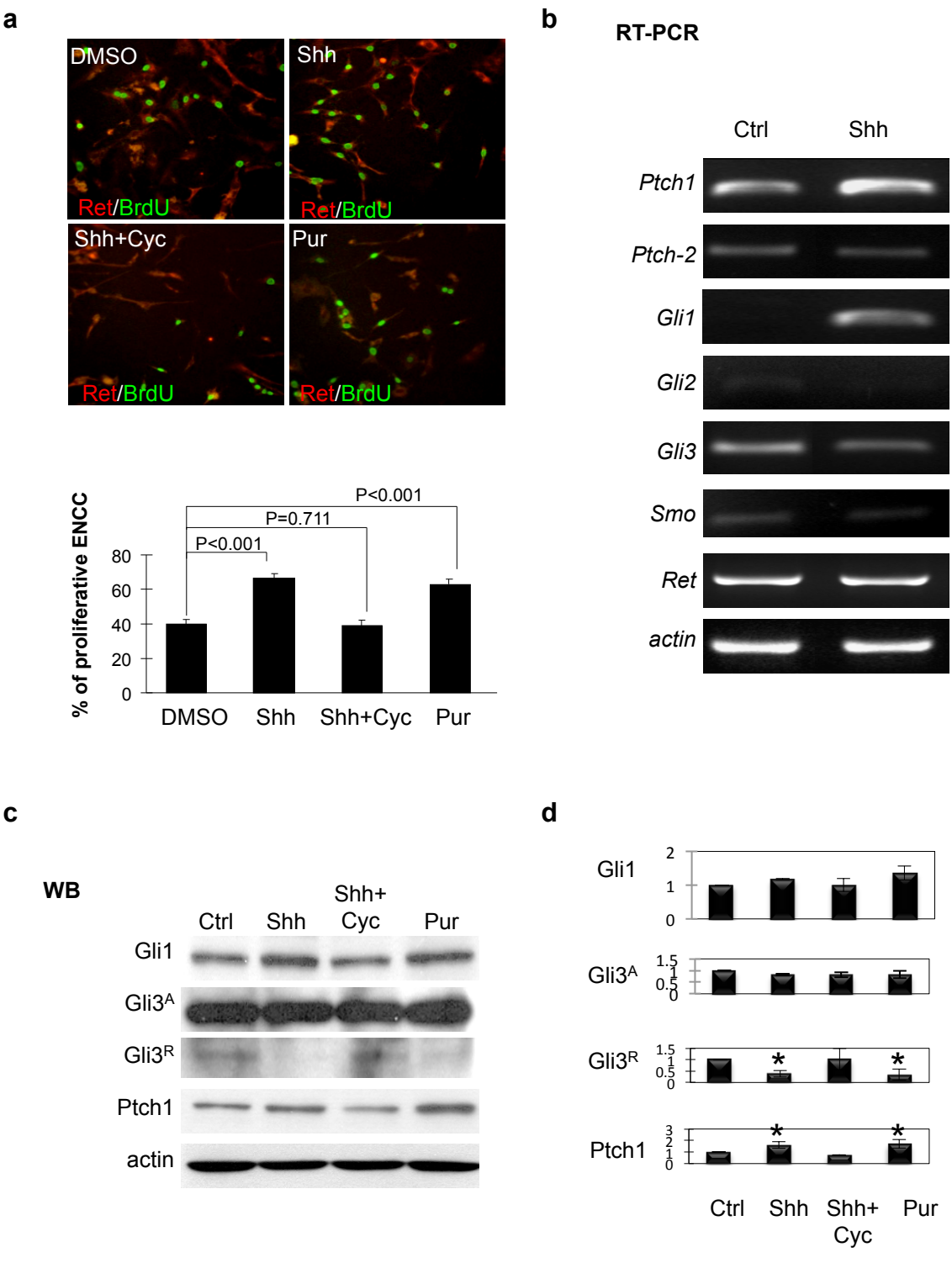
a
DMSO
Ret/BrdU
Shh
Ret/BrdU
Shh+Cyc
Ret/BrdU
Pur
Ret/BrdU
% of proliferative ENCC
P<0.001
P=0.711
P<0.001
80
60
40
20
0
DMSO
Shh
Shh+Cyc
Pur
b
RT-PCR
Ctrl
Shh
Ptch1
Ptch-2
Gli1
Gli2
Gli3
Smo
Ret
actin
c
WB
Ctrl
Shh
Shh+ Cyc
Pur
Gli1
Gli3A
Gli3R
Ptch1
actin
d
Gli1
2
1
0
Gli3A
1.5
1
0.5
0
Gli3R
1.5
1
0.5
0
*
*
Ptch1
3
2
1
0
*
*
Ctrl
Shh
Shh+ Cyc
Pur

Supplementary Figure 1. Shh promotes proliferation of ENCC by activation of Ptch-Smo-Gli pathway. (a) BrdU proliferation assay showed that Shh significantly increases the proliferation of ENCC progenitors (Ret^+), but not $Tuj1^+$ and $GFAP^+$ ENCCs (data not shown). This effect could be mimicked and counteracted by the treatments with purmorphamine (Pur, 1μM) and cyclopamine (Cyc, 0.5μM), respectively. ENCCs were treated with DMSO (vehicle control), Shh, purmorphamine (Pur) and cyclopamine (Cyc) for 3 days. BrdU (green) positive cells are proliferating. Cell proliferation rate was measured by the number of $BrdU^+/Ret^+$ cells over total number of Ret^+ cells. Bars represent the mean ± SEM and three independent experiments were performed. **(b)** RT-PCR analysis revealed high level of *Ptch1* and *Gli3*, a moderate level of *Ptch-2* and *Smo*, a low level of *Gli1* and *Gli2* in ENCC. Shh upregulated the expressions of *Ptch1* and *Gli1*. *Ret* and *β-actin* were served as the internal control. **(c)** Western blot analysis further confirmed that both Shh and its agonist, purmorphamine (Pur), upregulated the expressions of hedgehog target genes including Gli1 and Ptch1, and down-regulated the Gli3 repressor, which could be counteracted by the addition of the antagonist, cyclopamine (Cyc). Noteworthy, like in many other tissues, up-regulation of Gli3 activator was not observed upon the Shh and purmorphamine treatments, suggesting that it is not essential for the Shh-dependent cell proliferation. **(d)** Quantification of Western blots. Bars represent the mean ± SEM and three independent experiments were performed. *P*-values less than 0.05 were considered to be statistically significant different from the control (*).

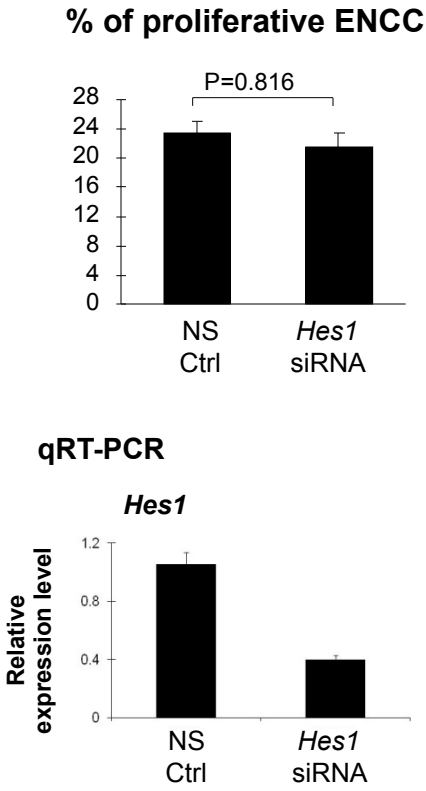

Supplementary Figure 2. Down-regulation of *Hes1* does not affect proliferation of ENCCs. (A) BrdU proliferation assay was performed to examine whether knockdown of *Hes1* affects the proliferation of ENCC progenitors. Proliferating cells were incorporated with BrdU and the relative proliferation rates were measured by counting proliferative ENCCs ($BrdU^+/Ret^+$) over the total number of ENCCs (Ret^+). The values reported in bar charts represent the mean ± SEM and three independent assays were performed. Data was analyzed by t-test. *P*-values less than 0.05 are statistically different from the control (Ctrl). **(B)** Quantitative RT-PCR on the expression of *Hes1* in ENCCs transfected with *Hes1* siRNA and non-silencing control (NS).

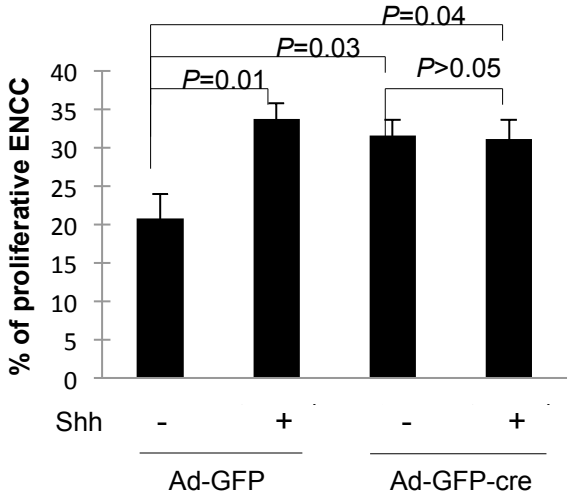

Supplementary Figure 3. *Ptch1* deletion is sufficient to fully activate hedgehog signaling. Relative proliferation rates were measured by counting $BrdU^+/Ret^+$ and total Ret^+ cells. The values reported in bar charts represent the mean ± SEM and three independent assays were performed. *P*-values less than 0.05 are statistically different

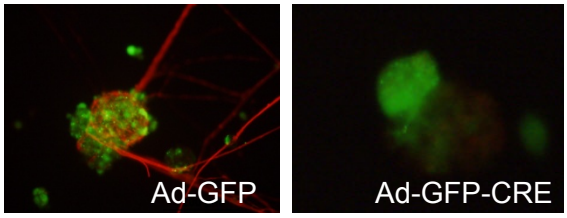

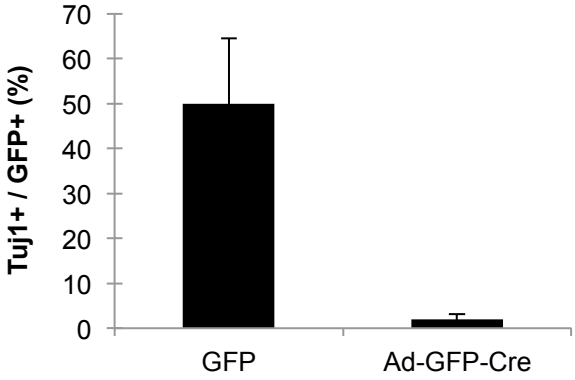

Supplementary Figure 4. Deletion of *Ptch1* inhibits neurogenesis of ENCCs. Immunocytochemistry: the control (Ad-GFP) and *Ptch1* deleted (Ad-GFP-CRE) cells were treated with GDNF for 10 days. **A.** Neuronal differentiation was monitored based on the expression of Neuronal Class III β-Tubulin (Tuj1). **B.** Percentage of neuronal precursors was measured over the total number of GFP^+ ENCCs. For each treatment group, a minimum of 6 random fields under 200X magnification with at least 250 cells in total was photographed for cell counting. The values reported in bar charts represent the mean ± SEM of three wells (i.e. 18 random fields).

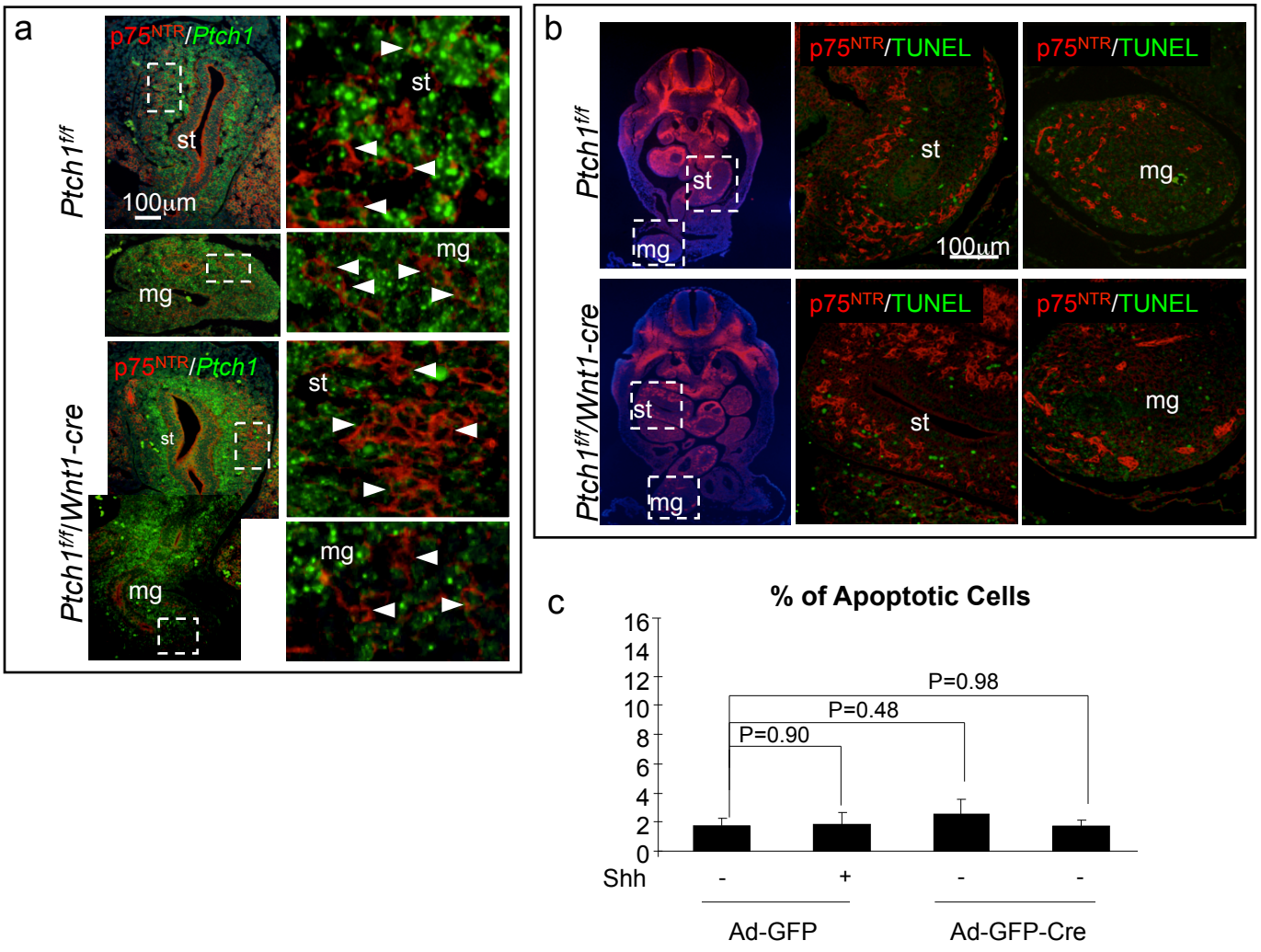

Supplementary Figure 5. Deletion of *Ptch1* in the pre-migratory ENCCs does not affect migration and cell survival. (a) *Ptch1*$^{-/-}$ ENCCs were detected in the mutant bowel (*Ptch1*$^{f/f}$*/Wnt1-Cre*). Transverse section through stomach (st) and midguts (mg) of E11.5 control (*Ptch1*$^{f/f}$) and *Ptch1* mutant (*Ptch1*$^{f/f}$*/Wnt1-Cre*) embryos stained for *Ptch1* transcript (green dots) by *in situ* hybridization and p75^{NTR} protein (Red) by immunostaining. *Ptch1* transcript were expressed in the mesenchyme and the ENCC progenitors (p75^{NTR+}) in control (*Ptch1*$^{f/f}$). *Ptch1* transcripts were specifically deleted in the ENCC progenitors of the mutants (*Ptch1*$^{f/f}$*/Wnt1-Cre*) but remained expressed in the mesenchyme. **(b)** Apoptosis of ENCC progenitors in E11.5 *Ptch1*$^{f/f}$ and conditional *Ptch1* knockout (*Ptch1*$^{f/f}$*/Wnt1-Cre*) guts were analyzed by TUNEL (green) and immunofluorescence for p75^{NTR} (red). ENCC progenitors (p75^{NTR+}, red) undergoing apoptosis (TUNEL^{+}, green) were rarely identified in both wildtype and mutant guts. Regions highlighted are magnified as shown either in insets (a) or on the right (b). Abbreviations: st, stomach; mg, midgut. **(c)** Deletion of *Ptch1* in ENCCs did not induce apoptosis. TUNEL assay was performed with *Ptch1*$^{f/f}$ ENCCs transduced with adenovirus expressing Cre recombinase (Ad-GFP-Cre) or control virus (Ad-GFP). Error bars indicated ± SEM across experimental replicates and three independent experiments were performed.

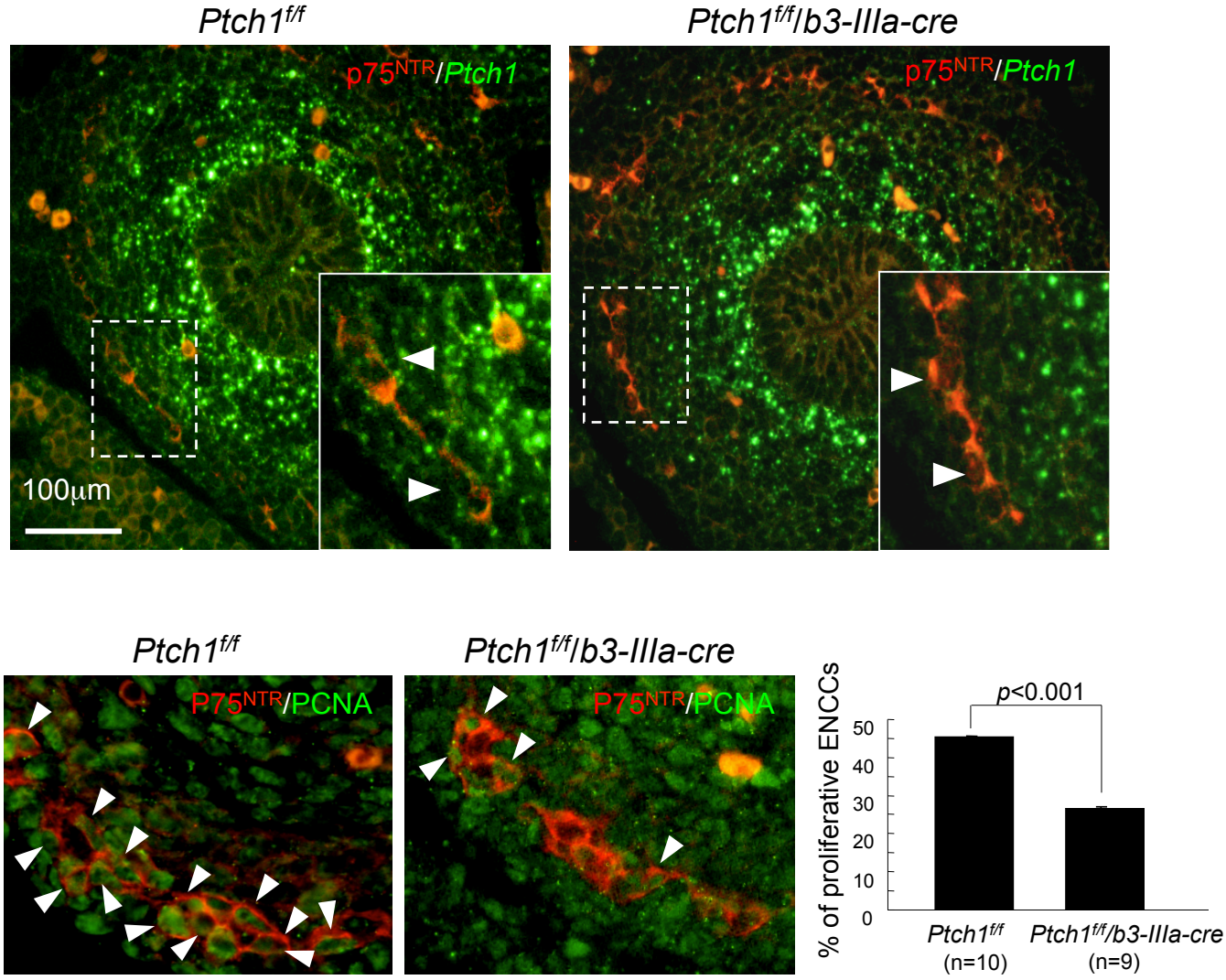

Supplementary Figure 6. Neural crest specific deletion of *Ptch1* in the *Ptch1$^{f/f}$/b3-IIIa-Cre* mouse embryonic guts. (A) Transverse section of E12.5 control (*Ptch1$^{f/f}$*) and *Ptch1* mutant (*Ptch1$^{f/f}$/b3-IIIa-Cre*) embryos stained for *Ptch1* transcript (green dots) by *in situ* hybridization and p75^{NTR} protein (Red) by immunostaining. *Ptch1* transcript were expressed in the mesenchyme and the ENCC progenitors (p75^{NTR+}) in control (*Ptch1$^{f/f}$*). *Ptch1* transcripts were specifically deleted in the ENCC progenitors of the mutants (*Ptch1$^{f/f}$/b3-IIIa-Cre*) but remained expressed in the mesenchyme. (Ptch1 negative ENCCs were found in the *Ptch1$^{f/f}$/b3-IIIa-Cre* embryos (arrowheads). Regions highlighted are magnified and shown as insets. **(B)** Proliferation of ENS progenitors in E12.5 control (*Ptch1$^{f/f}$*) and conditional *Ptch1* knockout (*Ptch1$^{f/f}$/b3-IIIa-Cre*) guts were analyzed by immunofluorescence for PCNA (green) and p75^{NTR} (red). Proliferating ENCCs (p75^{NTR+},PCNA^{+}, arrowheads) and non-proliferating ENCCs (p75^{NTR+}, PCNA^{-}) were identified and counted in control and mutant guts. The percentages of proliferative ENCCs in control and mutant guts were calculated and shown in bar-chart. Error bars indicated ± SEM across 10 control (*Ptch1$^{f/f}$*) and 9 mutant (*Ptch1$^{f/f}$/b3-IIIa-Cre*) mice.

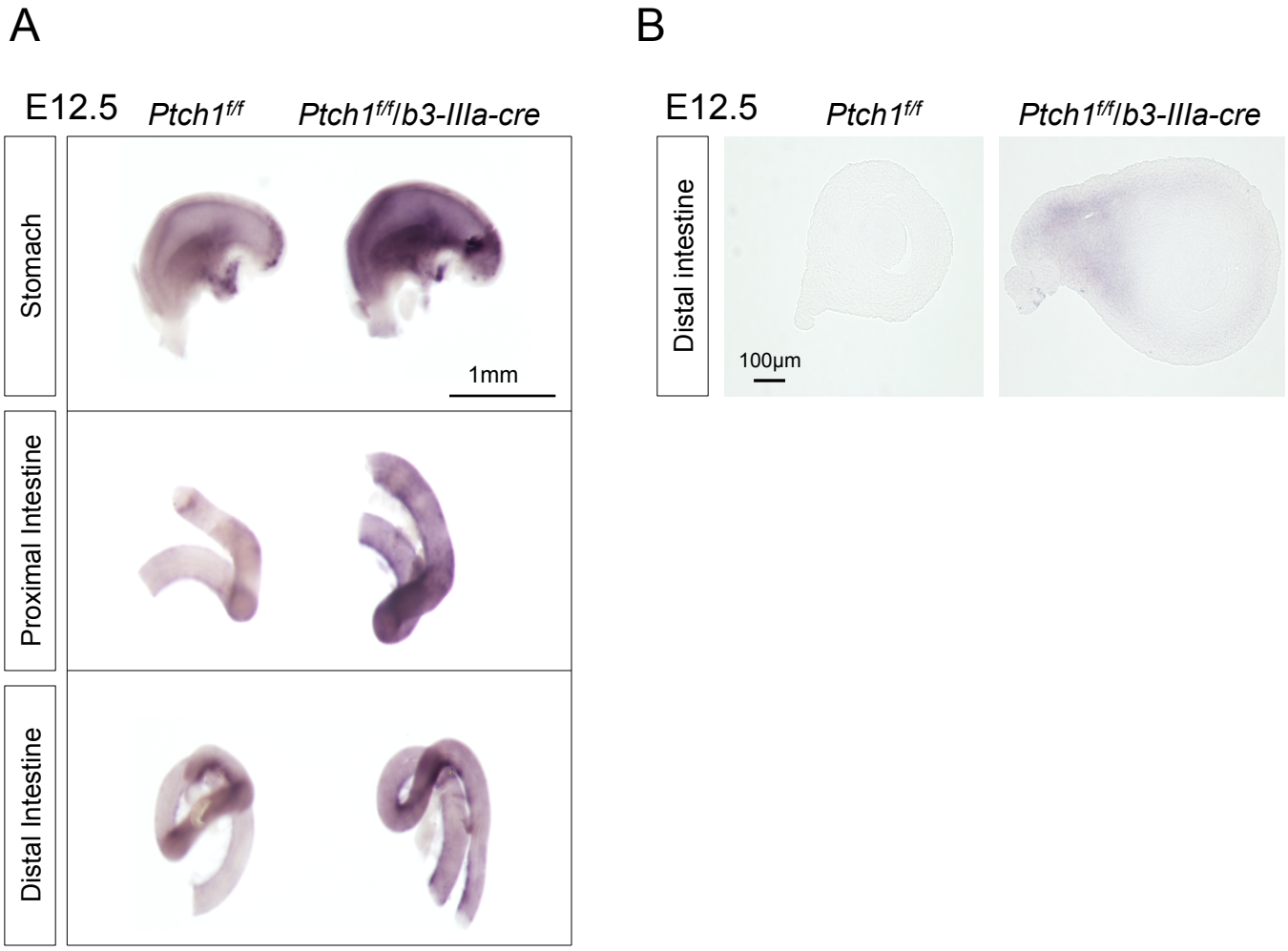

Supplementary Figure 7. Early detection of glial marker (*Fabp7*) in the *Ptch1$^{f/f}$/b3-IIIa-Cre* mutants. *In situ* hybridization was used to examine the expression of glial marker (*FABP7*) on E12.5 control (*Ptch1$^{f/f}$*) and conditional *Ptch1* knockout (*Ptch1$^{f/f}$/b3-IIIa-Cre*) guts. **(A)** The whole mount of the E12.5 control and *Ptch1* mutant bowels stained with *FABP7*. **(B)** Transverse sections of the E12.5 control and *Ptch1* mutant bowels stained with *FABP7*.

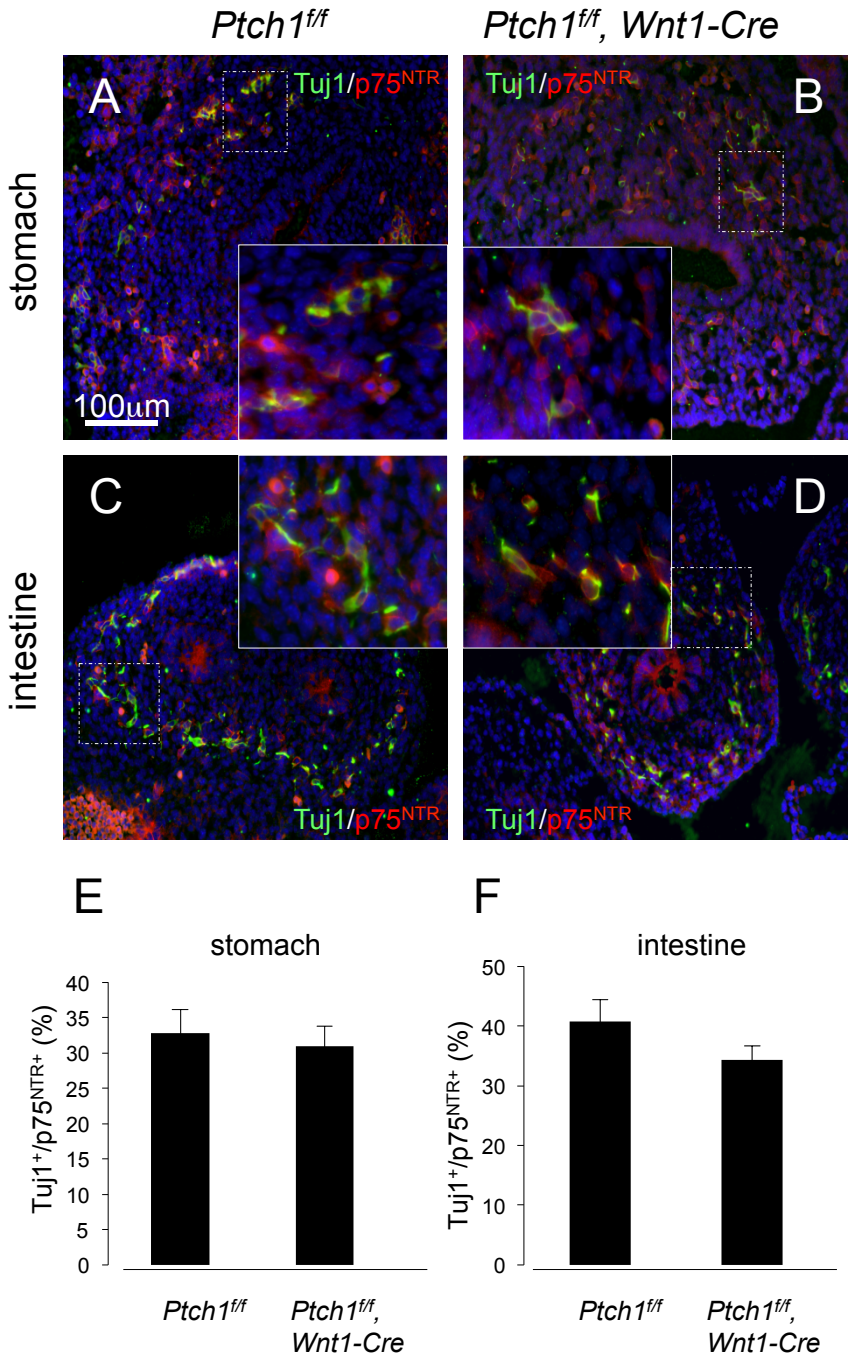

Supplementary Figure 8. No significant change in neuronal differentiation between control and *Ptch1* mutants. Immunohistochemical analysis of E11.5 control (**A & C**) and *Ptch1* mutant (*Ptch1*$^{f/f}$*/Wnt1-Cre*) (**B & D**) mouse embryos with anti-Tuj1 (green) and anti-p75^{NTR} (red) antibodies. Regions highlighted are magnified as shown in insets. Average percentages of Tuj1^{+} cells were measured by counting number of Tuj1^{+} cells over the total number of ENCCs (p75^{NTR+}) and data is shown with mean ± SEM (**E & F**). More than four sections from stomach or intestine regions of three different embryos were counted. Number of p75^{NTR+} ENCCs and the percentages of Tuj1^{+} cells in controls and mutants were comparable.

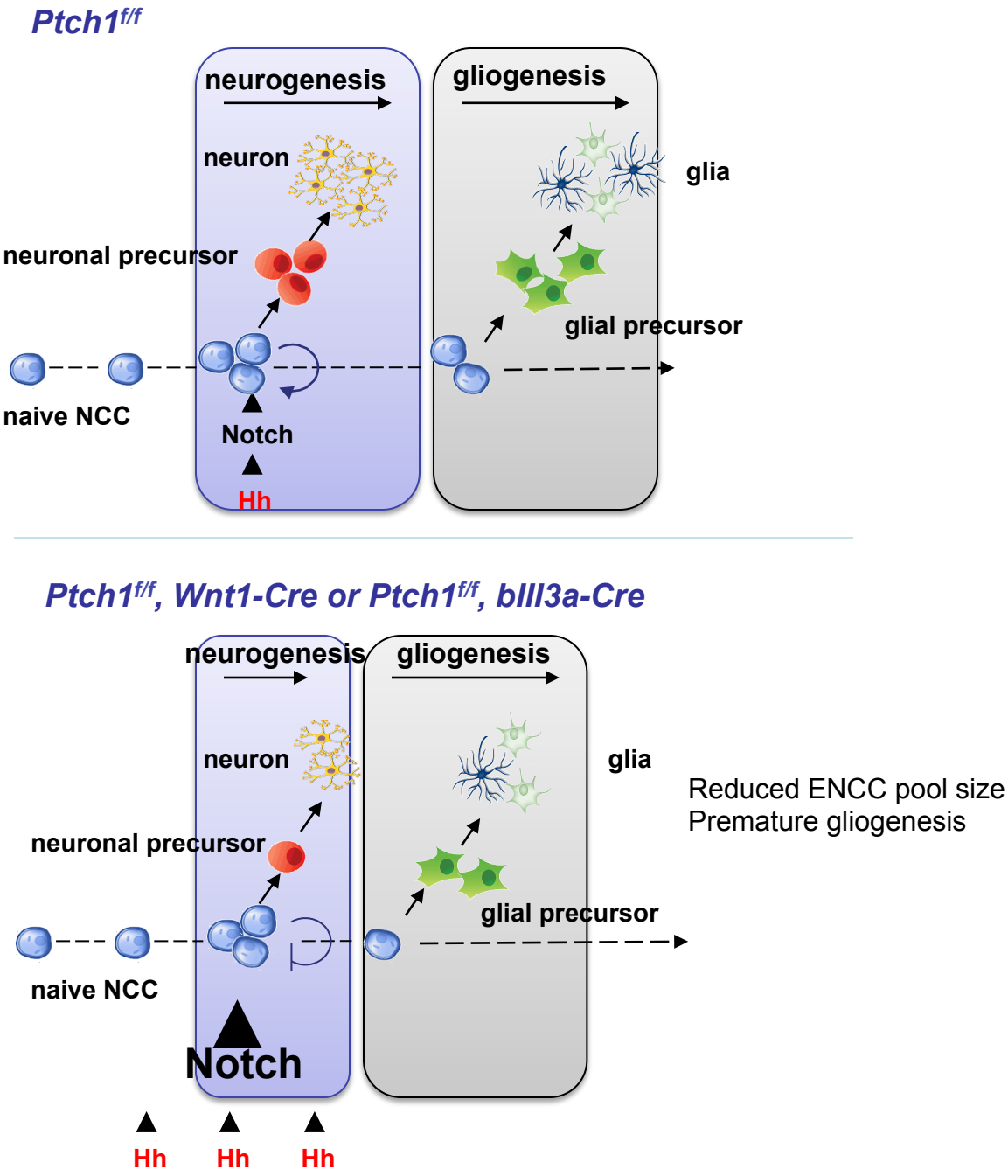

Supplementary Figure 9. Schematic diagram summarizes the potential functional interaction between Notch and Hh signalings during ENS development. Developmental process involves sequential waves of neurogenesis and gliogenesis, and requires an appropriate balance between the proliferation and differentiation of ENCCs and their progeny. Hh-Notch pathway mediates the pool size of ENCC progenitors by controlling their proliferation and switching neurogenesis to gliogenesis. Constitutive activation of Hh pathway in *Ptch1* mutant ENCCs results in robust induction of Notch signaling, leading to premature switch from neurogenesis to gliogenesis. Early ENCC differentiation may limit the expansion of ENCCs and result in a reduced ENCC pool size.

Supplementary table 1: Genes and number of SNPs in the two signaling gene sets

Pathway	Gene	Chromosome	Total length (bp)	No. of SNPs*
HH	*SHH*	7q36	9,410	2
	PTCH1	9q22.32	73,986	12
	GLI1	12q13.3	12,112	3
	GLI2	2q14	199,330	9
	GLI3	7p14	276,070	22
	SMO	7q32	24,674	6
	SUFU	10q24.32	129,446	6
NOTCH	*NOTCH1*	9q34	51,419	5
	NOTCH2	6q27	8,404	3
	NOTCH3	19p13.12	41,349	4
	DLL1	6q27	8,404	5
	DLL3	19q13.2	9,565	4
	DLL4	15q14	9,690	4
	JAG1	20p12.1	36,363	7
	JAG2	14q32.33	27,086	3
	MASH1	12q23.2	2,843	1
	HES1	3q29	2,440	7

* The SNP marker sets per gene were selected from the Affymetrix genotypes on basis of the linkage disequilibrium (LD) within the gene region. SNPs in perfect LD ($r^2 \geq 0.5$) were dropped from the analysis to avoid redundancy and minimize for multiple testing correction.

Supplementary Table 2: Differences in the first canonical correlation between case and controls

SHH / ***NOTCH***	*SHH*	***PTCH1***	*SMO*	*GLI1*	*GLI2*	*GLI3*	*SUFU*
NOTCH1	0.142	0.126	0.114	0.090	0.177	0.145	0.098
NOTCH2	0.186	0.106	0.141	0.026	0.084	0.186	0.020
NOTCH3	0.195	0.055	0.046	0.003	0.131	0.183	0.063
DLL1	0.049	0.132	0.049	0.101	0.143	0.203	0.143
DLL3	0.160	**0.321**	0.080	0.002	0.059	0.174	0.086
DLL4	0.076	0.072	0.112	-0.005	0.124	0.185	0.110
JAG1	-0.004	0.164	0.165	0.147	0.138	0.156	0.113
JAG2	0.099	0.105	0.150	0.051	0.051	0.114	0.107
MASH1	0.030	0.113	0.008	0.016	0.091	0.114	0.075
HES1	0.182	0.207	0.188	0.170	0.018	0.183	0.155